



Novel mixed finite element models for nonlinear analysis of plates

Abstract

In this study, mixed finite element models of plates bending are developed to include other variables (e.g., the membrane forces and shear forces) in addition to the generalized displacements to investigate their effect on nonlinear response. Various finite element models are developed using the weighted-residual statements of suitable equations. The classical plate theory and the first-order shear deformation plate theory are used in this study and the von Karman nonlinear strains are accounted for. Each newly developed model is examined and compared with displacement finite element models to evaluate their performance. Numerical results show that the new mixed models developed herein show better accuracy than existing displacement based models.

Keywords

Keywords ????????

Wooram Kim⁺ and
J. N. Reddy^{*}

Advanced Computational Mechanics Laboratory,
Department of Mechanical Engineering,
Texas A&M University, College Station, TX
77843-3123 – USA

Received xxx;
In revised form xxx

* Author email: basackdrs@hotmail.com

⁺currently at Department of Mechanical Engineering, Korea Army Academy at Yeong cheon, Yeong cheon, 770-849 South Korea

1 INTRODUCTION

The basic idea of mixed finite element model is to treat stresses or stress resultants as dependent unknowns in addition to the generalized displacements. Certain mixed finite element models of plates were developed more than two decades ago by Putchá and Reddy [3, 4] to overcome the drawbacks of the displacement based models. The mixed finite element models [3, 4] were developed in the past by including bending moments as independent variables to reduce the differentiability of the transverse displacement. The mixed models can provide the same level of accuracy for the bending moments as that for the displacements, whereas in the displacement based model the bending moments are calculated at points other than nodes in the post-processing. Thus, the displacement finite element models cannot provide the same level of accuracy for force-like variables as the mixed finite element models.

The objective of this study is to investigate the performance of finite element models based on weighted-residual formulations of the equations governing classical and first-order shear deformation plate theories. In particular, the study investigates merits and demerits of the newly developed mixed finite element models. The von Karman nonlinear equations [6, 9, 10]

18 are used to develop alternative finite element models to the conventional displacement-based
19 finite element models [5, 7, 8].

20 In the present study, mixed finite element models are developed to include other variables
21 (i.e., the membrane forces and shear forces) in addition to the bending moments, and to see
22 the effect of them on the nonlinear analysis. The effect of including other variables will be
23 compared with different mixed models to show the advantage of the one type of model over
24 other models. Two different mixed models based on the classical plate theory and two mixed
25 models based on the first-order shear deformation plate theory are developed. The performance
26 of the newly developed finite element models is evaluated by comparing the solutions with those
27 of the existing displacement finite element models [9, 10].

28 2 REVIEW OF PLATE THEORIES

29 Here we derive governing equations of the classical plate theory (CPT) and first-order shear
30 deformation theory (FSDT) of plates with the von Karman strains. The principle of virtual
31 displacements is used to derive the equilibrium equations in terms of the stress resultants and
32 then the stress resultants are expressed in terms of the displacements using elastic constitutive
33 relations. We only summarize the pertinent equations in this section without presenting the
34 details of the derivation.

35 The classical plate theory (CPT) is based on the Kirchhoff hypothesis, which consists
36 of the following three assumptions: (1) straight lines perpendicular to the mid-surface (i.e.
37 transverse normals) before deformation, remain straight after deformation; (2) the transverse
38 normals do not experience elongation (i.e. they are in-extensible); (3) the transverse normals
39 rotate such that they remain perpendicular to the mid-surface after deformation. On the
40 other hand, the first-order shear deformation plate theory (FSDT) is based on the assumption
41 the normals before deformation do not remain normal after deformation. Thus, the major
42 difference between the kinematics of the CPT and FSDT is that the normality condition of
43 CPT is relaxed in the FSDT, as illustrated in Fig. 1.

44 The equations of equilibrium expressed in terms of the stress resultants are the same in
45 both theories, and they are given by

$$\begin{aligned}
 & -\frac{\partial N_{xx}}{\partial x} - \frac{\partial N_{xy}}{\partial y} = 0, \\
 & -\frac{\partial N_{xy}}{\partial x} - \frac{\partial N_{yy}}{\partial y} = 0, \\
 & \frac{\partial}{\partial x} \left(N_{xx} \frac{\partial w_0}{\partial x} + N_{xy} \frac{\partial w_0}{\partial y} + Q_x \right) + \frac{\partial}{\partial y} \left(N_{xy} \frac{\partial w_0}{\partial x} + N_{yy} \frac{\partial w_0}{\partial y} + Q_y \right) + q(x) = 0, \\
 & Q_x - \left(\frac{\partial M_{xx}}{\partial x} + \frac{\partial M_{xy}}{\partial y} \right) = 0, \\
 & Q_y - \left(\frac{\partial M_{xy}}{\partial x} + \frac{\partial M_{yy}}{\partial y} \right) = 0.
 \end{aligned} \tag{1}$$

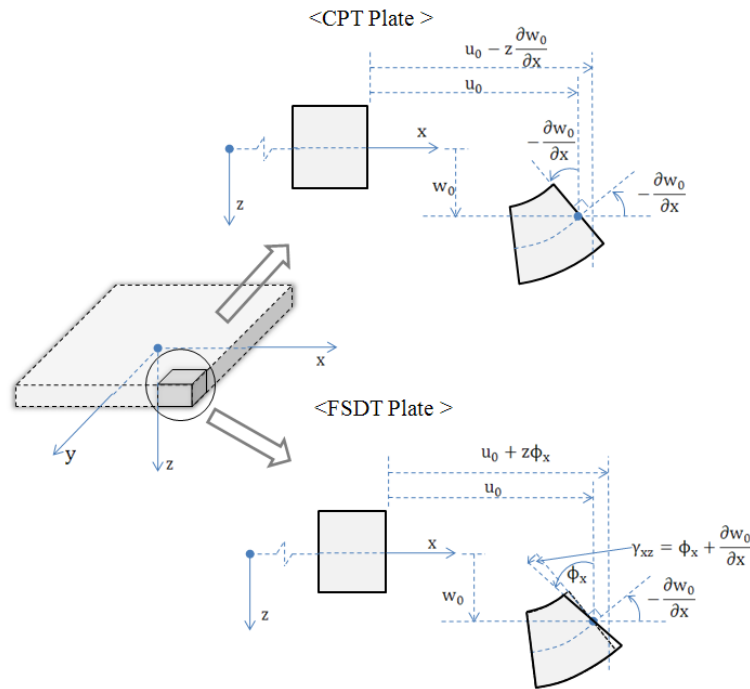


Figure 1 Undeformed and deformed edges in the CPT and FSDT theories (from [10]).

46 where the stress resultants are defined by

$$\begin{aligned}
 \begin{Bmatrix} N_{xx} \\ N_{yy} \\ N_{xy} \end{Bmatrix} &= \int_{-\frac{h}{2}}^{\frac{h}{2}} \begin{Bmatrix} \sigma_{xx} \\ \sigma_{yy} \\ \sigma_{xy} \end{Bmatrix} dz, \\
 \begin{Bmatrix} M_{xx} \\ M_{yy} \\ M_{xy} \end{Bmatrix} &= \int_{-\frac{h}{2}}^{\frac{h}{2}} \begin{Bmatrix} \sigma_{xx} \\ \sigma_{yy} \\ \sigma_{xy} \end{Bmatrix} z dz, \\
 \begin{Bmatrix} Q_y \\ Q_x \end{Bmatrix} &= \int_{-\frac{h}{2}}^{\frac{h}{2}} \begin{Bmatrix} yz \\ xz \end{Bmatrix} dz.
 \end{aligned} \tag{2}$$

47 Here h denotes the total thickness of the plate and the (x,y) -plane is taken to coincide
 48 with the middle plane of the plate and the z -coordinate is taken perpendicular to the plane of
 49 the plate. The difference in the kinematics of each plate theory is responsible for the difference
 50 in the relationships between the stress resultants and the generalized displacements.

51 2.1 The Classical Plate Theory

52 The displacement field of the CPT is given by

$$\begin{aligned}
u_1 &= u(x, y, z) = u_0(x, y) - z \left(\frac{\partial w_0(x, y)}{\partial x} \right), \\
u_2 &= v(x, y, z) = v_0(x, y) - z \left(\frac{\partial w_0(x, y)}{\partial y} \right), \\
u_3 &= w(x, y, z) = w_0(x, y).
\end{aligned} \tag{3}$$

53 Under the assumption of small strain but moderately large rotation, we can simplify the
54 components of the nonlinear strain tensor [6, 9, 10]. The components of the Green strain
55 tensor for this case, with the assumed displacement field in (3), are given by

$$\begin{aligned}
\varepsilon_{xx} &= \frac{\partial u_0}{\partial x} + \frac{1}{2} \left(\frac{\partial w_0}{\partial x} \right)^2 - z \frac{\partial^2 w_0}{\partial x^2}, \\
\varepsilon_{yy} &= \frac{\partial v_0}{\partial y} + \frac{1}{2} \left(\frac{\partial w_0}{\partial y} \right)^2 - z \frac{\partial^2 w_0}{\partial y^2}, \\
\varepsilon_{xy} &= \frac{1}{2} \left(\frac{\partial u_0}{\partial y} + \frac{\partial v_0}{\partial x} + \frac{\partial w_0}{\partial x} \frac{\partial w_0}{\partial y} - 2z \frac{\partial^2 w_0}{\partial x \partial y} \right).
\end{aligned} \tag{4}$$

56 We assume that the plate is made of linear elastic material and that the plane stress exists.
57 Then the plane stress-reduced elastic constitutive equations are given by

$$\begin{Bmatrix} \sigma_{xx} \\ \sigma_{yy} \\ \sigma_{xy} \end{Bmatrix} = \begin{bmatrix} Q_{11} & Q_{12} & 0 \\ Q_{12} & Q_{22} & 0 \\ 0 & 0 & Q_{66} \end{bmatrix} \begin{Bmatrix} \varepsilon_{xx} \\ \varepsilon_{yy} \\ 2\varepsilon_{xy} \end{Bmatrix}, \tag{5}$$

58 where the components of the elasticity matrix $[Q]$ are given by

$$\begin{aligned}
Q_{11} &= \frac{E_1}{1 - \nu_{12}\nu_{21}}, & Q_{12} &= \frac{\nu_{12}E_2}{1 - \nu_{12}\nu_{21}} = \frac{\nu_{21}E_1}{1 - \nu_{12}\nu_{21}}, \\
Q_{22} &= \frac{E_2}{1 - \nu_{12}\nu_{21}}, & Q_{66} &= G_{12}.
\end{aligned} \tag{6}$$

59 Here E_1 and E_2 denote the elastic moduli along the principal material coordinate directions,
60 which are assumed to coincide with the plate x and y -directions, ν_{12} and ν_{21} are Poisson's
61 ratios, and G_{12} is the shear modulus.

62 By using the constitutive relations given in Eq. (5) and the definitions of the resultants
63 given in the (2), we obtain the following plate constitutive relations:

$$\begin{aligned}
N_{xx} &= A_{11} \left[\frac{\partial u_0}{\partial x} + \frac{1}{2} \left(\frac{\partial w_0}{\partial x} \right)^2 \right] + A_{12} \left[\frac{\partial v_0}{\partial y} + \frac{1}{2} \left(\frac{\partial w_0}{\partial y} \right)^2 \right], \\
N_{yy} &= A_{12} \left[\frac{\partial u_0}{\partial x} + \frac{1}{2} \left(\frac{\partial w_0}{\partial x} \right)^2 \right] + A_{22} \left[\frac{\partial v_0}{\partial y} + \frac{1}{2} \left(\frac{\partial w_0}{\partial y} \right)^2 \right], \\
N_{xy} &= A_{66} \left(\frac{\partial u_0}{\partial y} + \frac{\partial v_0}{\partial x} + \frac{\partial w_0}{\partial x} \frac{\partial w_0}{\partial y} \right), \\
M_{xx} &= -D_{11} \left(\frac{\partial^2 w_0}{\partial x^2} \right) - D_{12} \left(\frac{\partial^2 w_0}{\partial y^2} \right), \\
M_{yy} &= -D_{12} \left(\frac{\partial^2 w_0}{\partial x^2} \right) - D_{22} \left(\frac{\partial^2 w_0}{\partial y^2} \right), \\
M_{xy} &= -2D_{66} \left(\frac{\partial^2 w_0}{\partial x \partial y} \right),
\end{aligned} \tag{7}$$

where the plate extensional and bending stiffnesses are defined as

$$(A_{ij}, D_{ij}) = \int_{-h/2}^{h/2} Q_{ij}(1, z) dz. \tag{8}$$

for $i, j = 1, 2, 6$.

2.2 The First Order Shear Deformation Theory

The displacement field of the FSDT is given by

$$\begin{aligned}
u_1 &= u(x, y, z) = u_0(x, y) + z\phi_x(x, y), \\
u_2 &= v(x, y, z) = v_0(x, y) + z\phi_y(x, y), \\
u_3 &= w_0(x, y).
\end{aligned} \tag{9}$$

The von Karman nonlinear strains of the FSDT are given by

$$\begin{aligned}
\varepsilon_{xx} &= \frac{\partial u_0}{\partial x} + \frac{1}{2} \left(\frac{\partial w_0}{\partial x} \right)^2 + z \frac{\partial \phi_x}{\partial x}, \\
\varepsilon_{yy} &= \frac{\partial v_0}{\partial y} + \frac{1}{2} \left(\frac{\partial w_0}{\partial y} \right)^2 + z \frac{\partial \phi_y}{\partial y}, \\
\varepsilon_{xy} &= \frac{1}{2} \left[\frac{\partial u_0}{\partial y} + \frac{\partial v_0}{\partial x} + \frac{\partial w_0}{\partial x} \frac{\partial w_0}{\partial y} + z \left(\frac{\partial \phi_x}{\partial y} + \frac{\partial \phi_y}{\partial x} \right) \right], \\
\varepsilon_{xz} &= \frac{\partial w_0}{\partial x} + \phi_x, \\
\varepsilon_{yz} &= \frac{\partial w_0}{\partial y} + \phi_y.
\end{aligned} \tag{10}$$

69 The plate constitutive equations in the FSDT are given by

$$\begin{aligned}
 N_{xx} &= A_{11} \left[\frac{\partial u_0}{\partial x} + \frac{1}{2} \left(\frac{\partial w_0}{\partial x} \right)^2 \right] + A_{12} \left[\frac{\partial v_0}{\partial y} + \frac{1}{2} \left(\frac{\partial w_0}{\partial y} \right)^2 \right], \\
 N_{yy} &= A_{12} \left[\frac{\partial u_0}{\partial x} + \frac{1}{2} \left(\frac{\partial w_0}{\partial x} \right)^2 \right] + A_{22} \left[\frac{\partial v_0}{\partial y} + \frac{1}{2} \left(\frac{\partial w_0}{\partial y} \right)^2 \right], \\
 N_{xy} &= A_{66} \left(\frac{\partial u_0}{\partial y} + \frac{\partial v_0}{\partial x} + \frac{\partial w_0}{\partial x} \frac{\partial w_0}{\partial y} \right), \\
 Q_x &= K_s A_{55} \left(\frac{\partial w_0}{\partial x} + \phi_x \right) \\
 Q_y &= K_s A_{44} \left(\frac{\partial w_0}{\partial y} + \phi_y \right) \\
 M_{xx} &= D_{11} \left(\frac{\partial \phi_x}{\partial x} \right) + D_{12} \left(\frac{\partial \phi_y}{\partial y} \right), \\
 M_{yy} &= D_{12} \left(\frac{\partial \phi_x}{\partial x} \right) + D_{22} \left(\frac{\partial \phi_y}{\partial y} \right), \\
 M_{xy} &= D_{66} \left(\frac{\partial \phi_x}{\partial y} + \frac{\partial \phi_y}{\partial x} \right), \tag{11}
 \end{aligned}$$

70 where, $K_s (= 5/6)$ is the shear correction factor. We introduce the effective shear forces as

$$\begin{aligned}
 V_x &= Q_x + \left(N_{xx} \frac{\partial w_0}{\partial x} + N_{xy} \frac{\partial w_0}{\partial y} \right), \\
 V_y &= Q_y + \left(N_{xy} \frac{\partial w_0}{\partial x} + N_{yy} \frac{\partial w_0}{\partial y} \right). \tag{12}
 \end{aligned}$$

71 3 FINITE ELEMENT MODELS

72 3.1 Summary of equations

73 In this section, we develop various types of the nonlinear mixed finite element models of plates.
 74 In current models, various stress resultants are included as independent nodal variables with
 75 the weighted-residual statements of suitable equations. Two new CPT models and two new
 76 FSDT models are developed. Keeping the forthcoming developments in mind the governing
 77 equations of the two theories are summarized first.

78 Governing equations of the CPT

$$\begin{aligned}
 &-\frac{\partial N_{xx}}{\partial x} - \frac{\partial N_{xy}}{\partial y} = 0, \\
 &-\frac{\partial N_{xy}}{\partial x} - \frac{\partial N_{yy}}{\partial y} = 0, \\
 &-\frac{\partial V_x}{\partial x} - \frac{\partial V_y}{\partial y} - q(x) = 0, \\
 &V_x - \left(\frac{\partial M_{xx}}{\partial x} + \frac{\partial M_{xy}}{\partial y} + N_{xx} \frac{\partial w_0}{\partial x} + N_{xy} \frac{\partial w_0}{\partial y} \right) = 0, \\
 &V_y - \left(\frac{\partial M_{xy}}{\partial x} + \frac{\partial M_{yy}}{\partial y} + N_{xy} \frac{\partial w_0}{\partial x} + N_{yy} \frac{\partial w_0}{\partial y} \right) = 0,
 \end{aligned} \tag{13}$$

79 and

$$\begin{aligned}
 &A_{11}^* N_{xx} + A_{12}^* N_{yy} = \left[\frac{\partial u_0}{\partial x} + \frac{1}{2} \left(\frac{\partial w_0}{\partial x} \right)^2 \right] \\
 &A_{12}^* N_{xx} + A_{22}^* N_{yy} = \left[\frac{\partial v_0}{\partial y} + \frac{1}{2} \left(\frac{\partial w_0}{\partial y} \right)^2 \right], \\
 &A_{66}^* N_{xy} = \left(\frac{\partial u_0}{\partial y} + \frac{\partial v_0}{\partial x} + \frac{\partial w_0}{\partial x} \frac{\partial w_0}{\partial y} \right), \\
 &D_{11}^* M_{xx} + D_{12}^* M_{yy} = - \left(\frac{\partial^2 w_0}{\partial x^2} \right), \\
 &D_{12}^* M_{xx} + D_{22}^* M_{yy} = - \left(\frac{\partial^2 w_0}{\partial y^2} \right), \\
 &D_{66}^* M_{xy} = -2 \left(\frac{\partial^2 w_0}{\partial x \partial y} \right).
 \end{aligned} \tag{14}$$

80 Governing equations of the FSDT

$$\begin{aligned}
 &-\frac{\partial N_{xx}}{\partial x} - \frac{\partial N_{xy}}{\partial y} = 0, \\
 &-\frac{\partial N_{xy}}{\partial x} - \frac{\partial N_{yy}}{\partial y} = 0, \\
 &\frac{\partial}{\partial x} \left(N_{xx} \frac{\partial w_0}{\partial x} + N_{xy} \frac{\partial w_0}{\partial y} + Q_x \right) + \frac{\partial}{\partial y} \left(N_{xy} \frac{\partial w_0}{\partial x} + N_{yy} \frac{\partial w_0}{\partial y} + Q_y \right) + q(x) = 0, \\
 &Q_x - \left(\frac{\partial M_{xx}}{\partial x} + \frac{\partial M_{xy}}{\partial y} \right) = 0, \\
 &Q_y - \left(\frac{\partial M_{xy}}{\partial x} + \frac{\partial M_{yy}}{\partial y} \right) = 0,
 \end{aligned} \tag{15}$$

81 and

$$\begin{aligned}
 A_{11}^* N_{xx} + A_{12}^* N_{yy} &= \left[\frac{\partial u_0}{\partial x} + \frac{1}{2} \left(\frac{\partial w_0}{\partial x} \right)^2 \right], \\
 A_{12}^* N_{xx} + A_{22}^* N_{yy} &= \left[\frac{\partial v_0}{\partial y} + \frac{1}{2} \left(\frac{\partial w_0}{\partial y} \right)^2 \right], \\
 A_{66}^* N_{xy} &= \left(\frac{\partial u_0}{\partial y} + \frac{\partial v_0}{\partial x} + \frac{\partial w_0}{\partial x} \frac{\partial w_0}{\partial y} \right), \\
 0 &= -\frac{Q_x}{K_s A_{55}} + \left(\frac{\partial w_0}{\partial x} + \phi_x \right), \\
 0 &= -\frac{Q_y}{K_s A_{44}} + \left(\frac{\partial w_0}{\partial y} + \phi_y \right), \\
 D_{11}^* M_{xx} + D_{12}^* M_{yy} &= \left(\frac{\partial \phi_x}{\partial x} \right), \\
 D_{12}^* M_{xx} + D_{22}^* M_{yy} &= \left(\frac{\partial \phi_y}{\partial y} \right), \\
 D_{66}^* M_{xy} &= \left(\frac{\partial \phi_x}{\partial y} + \frac{\partial \phi_y}{\partial x} \right).
 \end{aligned} \tag{16}$$

82 where A_{ij}^* and D_{ij}^* are inverses of the stiffness matrices: $\mathbf{A}^* = \mathbf{A}^{-1}$ and $\mathbf{D}^* = \mathbf{D}^{-1}$.

83 **3.2 Finite Element Model I (CPT)**

84 In this mixed finite model of the CPT, eleven variables, $u_0, v_0, w_0, N_{xx}, N_{yy}, N_{xy}, V_x, V_y,$
 85 M_{xx}, M_{yy} and M_{xy} , are treated as independent variables. The following weighed-residual
 86 statements are used:

$$\begin{aligned}
 \int_{\Omega_e} \left(\frac{\partial \bar{W}_1}{\partial x} N_{xx}^a + \frac{\partial \bar{W}_1}{\partial y} N_{xy}^a \right) dx dy - \oint_{\Gamma_e} \bar{W}_1 \{ n_x N_{xx} + n_y N_{xy} \} ds &= 0, \\
 \int_{\Omega_e} \left(\frac{\partial \bar{W}_2}{\partial x} N_{xy}^a + \frac{\partial \bar{W}_2}{\partial y} N_{yy}^a \right) dx dy - \oint_{\Gamma_e} \bar{W}_2 \{ n_x N_{xy} + n_y N_{yy} \} ds &= 0, \\
 \int_{\Omega_e} \left(\frac{\partial \bar{W}_3}{\partial x} V_x^a + \frac{\partial \bar{W}_3}{\partial y} V_y^a - \bar{W}_3 q(x) \right) dx dy - \oint_{\Gamma_e} \bar{W}_3 \{ n_x V_x + n_y V_y \} ds &= 0, \\
 \int_{\Omega_e} \bar{W}_4 \left\{ -A_{11}^* N_{xx}^a - A_{12}^* N_{yy}^a + \left[\frac{\partial u_0^a}{\partial x} + \frac{1}{2} \left(\frac{\partial w_0^a}{\partial x} \right)^2 \right] \right\} dx dy &= 0, \\
 \int_{\Omega_e} \bar{W}_5 \left\{ -A_{12}^* N_{xx}^a - A_{22}^* N_{yy}^a + \left[\frac{\partial v_0^a}{\partial y} + \frac{1}{2} \left(\frac{\partial w_0^a}{\partial y} \right)^2 \right] \right\} dx dy &= 0, \\
 \int_{\Omega_e} \bar{W}_6 \left[-A_{66}^* N_{xy}^a + \left(\frac{\partial u_0^a}{\partial y} + \frac{\partial v_0^a}{\partial x} + \frac{1}{2} \frac{\partial w_0^a}{\partial x} \frac{\partial w_0^a}{\partial y} + \frac{1}{2} \frac{\partial w_0^a}{\partial x} \frac{\partial w_0^a}{\partial y} \right) \right] dx dy &= 0,
 \end{aligned}$$

$$\begin{aligned}
 & \int_{\Omega_e} \bar{W}_7 \left(-V_x^a + \frac{\partial M_{xx}^a}{\partial x} + \frac{\partial M_{xy}^a}{\partial y} + N_{xx}^a \frac{\partial w_0^a}{\partial x} + N_{xy}^a \frac{\partial w_0^a}{\partial y} \right) dx dy = 0, \\
 & \int_{\Omega_e} \bar{W}_8 \left(-V_y^a + \frac{\partial M_{xy}^a}{\partial x} + \frac{\partial M_{yy}^a}{\partial y} + N_{xy}^a \frac{\partial w_0^a}{\partial x} + N_{yy}^a \frac{\partial w_0^a}{\partial y} \right) dx dy = 0, \\
 & \int_{\Omega_e} \left(-D_{11}^* \bar{W}_9 M_{xx}^a - D_{12}^* \bar{W}_9 M_{yy}^a + \frac{\partial \bar{W}_9}{\partial x} \frac{\partial w_0^a}{\partial x} \right) dx dy - \int_{\Gamma_e} \bar{W}_9 \left(n_x \frac{\partial w_0}{\partial x} \right) ds = 0, \\
 & \int_{\Omega_e} \left(-D_{12}^* \bar{W}_{10} M_{xx}^a - D_{22}^* \bar{W}_{10} M_{yy}^a + \frac{\partial \bar{W}_{10}}{\partial y} \frac{\partial w_0^a}{\partial y} \right) dx dy - \int_{\Gamma_e} \bar{W}_{10} \left(n_y \frac{\partial w_0}{\partial y} \right) ds = 0, \\
 & \int_{\Omega_e} \left(-D_{66}^* \bar{W}_{11} M_{xy}^a + \frac{\partial \bar{W}_{11}}{\partial x} \frac{\partial w_0^a}{\partial y} + \frac{\partial \bar{W}_{11}}{\partial y} \frac{\partial w_0^a}{\partial x} \right) dx dy \\
 & \quad - \int_{\Gamma_e} \bar{W}_{11} \left(n_x \frac{\partial w_0}{\partial y} + n_y \frac{\partial w_0}{\partial x} \right) ds = 0. \tag{17}
 \end{aligned}$$

87 where, Γ_e is the boundary of a typical element region Ω_e , variables with a superscript ‘a’ denote
 88 the approximated variables, and n_x and n_y denote the x and y components (i.e. direction
 89 cosines) of the unit normal vector on the boundary. The primary variables and the secondary
 90 variable of the formulation are as follows.

Primary variables	Secondary variables
u_0	$n_x N_{xx} + n_y N_{xy}$
v_0	$n_x N_{xy} + n_y N_{yy}$
w_0	$n_x V_x + n_y V_y$
M_{xx}	$n_x \frac{\partial w_0}{\partial x}$
M_{yy}	$n_y \frac{\partial w_0}{\partial y}$
M_{xy}	$n_x \frac{\partial w_0}{\partial y} + n_y \frac{\partial w_0}{\partial x}$

92 With the weighted residual statements in (17), we can develop the finite element model,
 93 denoted as Model I, of the CPT by approximating the 11 variables with known interpolation
 94 functions and unknown nodal values. The Lagrange interpolation functions are admissible for
 95 all variables (i.e., C^0 continuity of all variables is required). We take

$$\begin{aligned}
 u_0 & \cong u_0^a = \sum_{j=1}^m \psi_j^{u_0}(x, y) u_j, & \bar{W}_1 & = \psi_i^{u_0}(x, y), \\
 v_0 & \cong v_0^a = \sum_{j=1}^m \psi_j^{v_0}(x, y) v_j, & \bar{W}_2 & = \psi_i^{v_0}(x, y), \\
 w_0 & \cong w_0^a = \sum_{j=1}^n \psi_j^{w_0}(x, y) w_j, & \bar{W}_3 & = \psi_i^{w_0}(x, y), \\
 N_{xx} & \cong N_{xx}^a = \sum_{j=1}^p \psi_j^{N_{xx}}(x, y) N_j^1, & \bar{W}_4 & = \psi_i^{N_{xx}}(x, y),
 \end{aligned}$$

$$\begin{aligned}
 N_{yy} &\cong N_{yy}^a = \sum_{j=1}^p \psi_j^{N_{yy}}(x, y) \mathbb{N}_j^2, & \bar{W}_5 &= \psi_i^{N_{yy}}(x, y), \\
 N_{xy} &\cong N_{xy}^a = \sum_{j=1}^p \psi_j^{N_{xy}}(x, y) \mathbb{N}_j^3, & \bar{W}_6 &= \psi_i^{N_{xy}}(x, y), \\
 V_x &\cong V_x^a = \sum_{j=1}^q \psi_j^{V_x}(x, y) \mathbb{V}_j^1, & \bar{W}_7 &= \psi_i^{V_x}(x, y), \\
 V_y &\cong V_y^a = \sum_{j=1}^q \psi_j^{V_y}(x, y) \mathbb{V}_j^2, & \bar{W}_8 &= \psi_i^{V_y}(x, y), \\
 M_{xx} &\cong M_{xx}^a = \sum_{j=1}^r \psi_j^{M_{xx}}(x, y) \mathbb{M}_j^1, & \bar{W}_9 &= \psi_i^{M_{xx}}(x, y), \\
 M_{yy} &\cong M_{yy}^a = \sum_{j=1}^r \psi_j^{M_{yy}}(x, y) \mathbb{M}_j^2, & \bar{W}_{10} &= \psi_i^{M_{yy}}(x, y), \\
 M_{xy} &\cong M_{xy}^a = \sum_{j=1}^r \psi_j^{M_{xy}}(x, y) \mathbb{M}_j^3, & \bar{W}_{11} &= \psi_i^{M_{xy}}(x, y). \tag{18}
 \end{aligned}$$

96 By substituting the expressions from (18) into the weighted-residual statements of (17),
 97 we obtain the finite element equations

$$\begin{bmatrix} [K^{(1)(1)}] & \dots & [K^{(1)(6)}] & \dots & [K^{(1)(11)}] \\ \vdots & \ddots & \vdots & \ddots & \vdots \\ [K^{(6)(1)}] & \dots & [K^{(6)(6)}] & \dots & [K^{(6)(11)}] \\ \vdots & \ddots & \vdots & \ddots & \vdots \\ [K^{(11)(1)}] & \dots & [K^{(11)(6)}] & \dots & [K^{(11)(11)}] \end{bmatrix} \begin{Bmatrix} \{u_j\} \\ \vdots \\ \{\mathbb{N}_j^3\} \\ \vdots \\ \{\mathbb{M}_j^3\} \end{Bmatrix} = \begin{Bmatrix} \{F^{(1)}\} \\ \vdots \\ \{F^{(6)}\} \\ \vdots \\ \{F^{(11)}\} \end{Bmatrix} . \tag{19}$$

98 where

$$\begin{aligned}
 [K^{14}] &= \int_{\Omega_e} \left\{ \frac{\partial \psi_i^{u_0}}{\partial x} \psi_j^{N_{xx}} \right\} dx dy, & [K^{16}] &= \int_{\Omega_e} \left\{ \frac{\partial \psi_i^{u_0}}{\partial y} \psi_j^{N_{xy}} \right\} dx dy, \\
 [K^{25}] &= \int_{\Omega_e} \left\{ \frac{\partial \psi_i^{v_0}}{\partial y} \psi_j^{N_{yy}} \right\} dx dy, & [K^{26}] &= \int_{\Omega_e} \left\{ \frac{\partial \psi_i^{v_0}}{\partial x} \psi_j^{N_{xy}} \right\} dx dy, \\
 [K^{37}] &= \int_{\Omega_e} \left\{ \frac{\partial \psi_i^{w_0}}{\partial x} \psi_j^{V_x} \right\} dx dy, & [K^{38}] &= \int_{\Omega_e} \left\{ \frac{\partial \psi_i^{w_0}}{\partial y} \psi_j^{V_y} \right\} dx dy, \\
 [K^{41}] &= \int_{\Omega_e} \left\{ \psi_i^{N_{xx}} \frac{\partial \psi_j^{u_0}}{\partial x} \right\} dx dy, & [K^{43}] &= \int_{\Omega_e} \left\{ \frac{1}{2} \left(\frac{\partial \mathbf{w}_0^a}{\partial \mathbf{x}} \right) \psi_i^{N_{xx}} \frac{\partial \psi_j^{w_0}}{\partial x} \right\} dx dy \\
 [K^{44}] &= \int_{\Omega_e} \left\{ -A_{11}^* \psi_i^{N_{xx}} \psi_j^{N_{xx}} \right\} dx dy, & [K^{45}] &= \int_{\Omega_e} \left\{ -A_{12}^* \psi_i^{N_{xx}} \psi_j^{N_{yy}} \right\} dx dy, \\
 [K^{52}] &= \int_{\Omega_e} \left\{ \psi_i^{N_{yy}} \frac{\partial \psi_j^{v_0}}{\partial y} \right\} dx dy, & [K^{53}] &= \int_{\Omega_e} \left\{ \frac{1}{2} \left(\frac{\partial \mathbf{w}_0^a}{\partial \mathbf{y}} \right) \psi_i^{N_{yy}} \frac{\partial \psi_j^{w_0}}{\partial y} \right\} dx dy,
 \end{aligned}$$

$$\begin{aligned}
 [K^{54}] &= \int_{\Omega_e} \left\{ -A_{12}^* \psi_i^{N_{yy}} \psi_j^{N_{xx}} \right\} dx dy, & [K^{55}] &= \int_{\Omega_e} \left\{ -A_{22}^* \psi_i^{N_{yy}} \psi_j^{N_{yy}} \right\} dx dy, \\
 [K^{61}] &= \int_{\Omega_e} \left\{ \psi_i^{N_{xy}} \frac{\partial \psi_j^{w_0}}{\partial y} \right\} dx dy, & [K^{62}] &= \int_{\Omega_e} \left\{ \psi_i^{N_{xy}} \frac{\partial \psi_j^{v_0}}{\partial x} \right\} dx dy, \\
 [K^{66}] &= \int_{\Omega_e} \left\{ -A_{66}^* \psi_i^{N_{xy}} \psi_j^{N_{xy}} \right\} dx dy, \\
 [K^{63}] &= \int_{\Omega_e} \left\{ \frac{1}{2} \left[\left(\frac{\partial \mathbf{w}_0^a}{\partial \mathbf{x}} \right) \psi_i^{N_{xy}} \frac{\partial \psi_j^w}{\partial y} + \left(\frac{\partial \mathbf{w}_0^a}{\partial \mathbf{y}} \right) \psi_i^{N_{xy}} \frac{\partial \psi_j^w}{\partial x} \right] \right\} dx dy, \\
 [K^{74}] &= \int_{\Omega_e} \left\{ \left(\frac{\partial \mathbf{w}_0^a}{\partial \mathbf{x}} \right) \psi_i^{V_x} \psi_j^{N_{xx}} \right\} dx dy, & [K^{76}] &= \int_{\Omega_e} \left\{ \left(\frac{\partial \mathbf{w}_0^a}{\partial \mathbf{y}} \right) \psi_i^{V_x} \psi_j^{N_{xy}} \right\} dx dy, \\
 [K^{77}] &= \int_{\Omega_e} \left\{ -\psi_i^{V_x} \psi_j^{V_x} \right\} dx dy, & [K^{79}] &= \int_{\Omega_e} \left\{ \psi_i^{V_x} \frac{\partial \psi_j^{M_{xx}}}{\partial x} \right\} dx dy, \\
 [K^{7(11)}] &= \int_{\Omega_e} \left\{ \psi_i^{V_x} \frac{\partial \psi_j^{M_{xy}}}{\partial y} \right\} dx dy, \\
 [K^{85}] &= \int_{\Omega_e} \left\{ \left(\frac{\partial \mathbf{w}_0^a}{\partial \mathbf{y}} \right) \psi_i^{V_y} \psi_j^{N_{yy}} \right\} dx dy, & [K^{86}] &= \int_{\Omega_e} \left\{ \left(\frac{\partial \mathbf{w}_0^a}{\partial \mathbf{x}} \right) \psi_i^{V_y} \psi_j^{N_{xy}} \right\} dx dy, \\
 [K^{88}] &= \int_{\Omega_e} \left\{ -\psi_i^{V_y} \psi_j^{V_y} \right\} dx dy, & [K^{8(10)}] &= \int_{\Omega_e} \left\{ \psi_i^{V_y} \frac{\partial \psi_j^{M_{yy}}}{\partial y} \right\} dx dy, \\
 [K^{8(11)}] &= \int_{\Omega_e} \left\{ \psi_i^{V_y} \frac{\partial \psi_j^{M_{xy}}}{\partial x} \right\} dx dy, \\
 [K^{93}] &= \int_{\Omega_e} \left\{ \frac{\partial \psi_i^{M_{xx}}}{\partial x} \frac{\partial \psi_j^{w_0}}{\partial x} \right\} dx dy, & [K^{99}] &= \int_{\Omega_e} \left\{ -D_{11}^* \psi_i^{M_{xx}} \psi_j^{M_{xx}} \right\} dx dy, \\
 [K^{9(10)}] &= \int_{\Omega_e} \left\{ -D_{12}^* \psi_i^{M_{xx}} \psi_j^{M_{yy}} \right\} dx dy \\
 [K^{(10)3}] &= \int_{\Omega_e} \left\{ \frac{\partial \psi_i^{M_{xx}}}{\partial y} \frac{\partial \psi_j^{w_0}}{\partial y} \right\} dx dy, & [K^{(10)9}] &= \int_{\Omega_e} \left\{ -D_{12}^* \psi_i^{M_{yy}} \psi_j^{M_{xx}} \right\} dx dy, \\
 [K^{(10)(10)}] &= \int_{\Omega_e} \left\{ -D_{22}^* \psi_i^{M_{yy}} \psi_j^{M_{yy}} \right\} dx dy, \\
 [K^{(11)3}] &= \int_{\Omega_e} \left\{ \frac{\partial \psi_i^{M_{xy}}}{\partial x} \frac{\partial \psi_j^{w_0}}{\partial y} + \frac{\partial \psi_i^{M_{xy}}}{\partial y} \frac{\partial \psi_j^{w_0}}{\partial x} \right\} dx dy, \\
 [K^{(11)(11)}] &= \int_{\Omega_e} \left\{ -D_{66}^* \psi_i^{M_{xy}} \psi_j^{M_{xy}} \right\} dx dy. \\
 \{F^1\} &= \oint_{\Gamma_e} \psi_i^u \{n_x N_{xx} + n_y N_{xy}\} ds, & \{F^2\} &= \oint_{\Gamma_e} \psi_i^v \{n_x N_{xy} + n_y N_{yy}\} ds, \\
 \{F^3\} &= \int_{\Omega_e} \{\psi_i^w q(x)\} dx dy + \oint_{\Gamma_e} \psi_i^w Q_n ds & \{F^9\} &= \oint_{\Gamma_e} \psi_i^{M_{xx}} \left(\frac{\partial w_0}{\partial x} n_x \right) ds,
 \end{aligned}$$

$$\begin{aligned} \{F^{(10)}\} &= \oint_{\Gamma_e} \psi_i^{M_{yy}} \left(\frac{\partial w_0}{\partial y} n_y \right) ds, \\ \{F^{(11)}\} &= \oint_{\Gamma_e} \left\{ \psi_i^{M_{xy}} \left(\frac{\partial w_0}{\partial y} n_x + \frac{\partial w_0}{\partial x} n_y \right) \right\} ds. \end{aligned} \quad (20)$$

99 The rest of the coefficients matrices and force vectors are zero.

100 3.3 Finite Element Model II (CPT)

101 The shear forces V_x and V_y can be eliminated by substituting the forth and the fifth equilib-
 102 rium equations into the third equilibrium equation of the CPT. Following 9 weighted-residual
 103 statements are used:

$$\begin{aligned} &\int_{\Omega_e} \left(\frac{\partial \bar{W}_1}{\partial x} N_{xx}^a + \frac{\partial \bar{W}_1}{\partial y} N_{xy}^a \right) dx dy - \oint_{\Gamma_e} \bar{W}_1 \{n_x N_{xx} + n_y N_{xy}\} ds = 0, \\ &\int_{\Omega_e} \left(\frac{\partial \bar{W}_2}{\partial x} N_{xy}^a + \frac{\partial \bar{W}_2}{\partial y} N_{yy}^a \right) dx dy - \oint_{\Gamma_e} \bar{W}_2 \{n_x N_{xy} + n_y N_{yy}\} ds = 0, \\ &\int_{\Omega_e} \left\{ \frac{\partial \bar{W}_3}{\partial x} \left(\frac{\partial M_{xx}^a}{\partial x} + \frac{\partial M_{xy}^a}{\partial y} + N_{xx}^a \frac{\partial w_0^a}{\partial x} + N_{xy}^a \frac{\partial w_0^a}{\partial y} \right) \right. \\ &\quad \left. + \frac{\partial \bar{W}_3}{\partial y} \left(\frac{\partial M_{xy}^a}{\partial x} + \frac{\partial M_{yy}^a}{\partial y} + N_{xy}^a \frac{\partial w_0^a}{\partial x} + N_{yy}^a \frac{\partial w_0^a}{\partial y} \right) - \bar{W}_3 q(x) \right\} dx dy \\ &\quad - \oint_{\Gamma_e} \bar{W}_3 \{n_x V_x + n_y V_y\} ds = 0, \\ &\int_{\Omega_e} \bar{W}_4 \left\{ -A_{11}^* N_{xx}^a - A_{12}^* N_{yy}^a + \left[\frac{\partial u_0^a}{\partial x} + \frac{1}{2} \left(\frac{\partial w_0^a}{\partial x} \right)^2 \right] \right\} dx dy = 0 \\ &\int_{\Omega_e} \bar{W}_5 \left\{ -A_{12}^* N_{xx}^a - A_{22}^* N_{yy}^a + \left[\frac{\partial v_0^a}{\partial y} + \frac{1}{2} \left(\frac{\partial w_0^a}{\partial y} \right)^2 \right] \right\} dx dy = 0, \\ &\int_{\Omega_e} \bar{W}_6 \left[-A_{66}^* N_{xy}^a + \left(\frac{\partial u_0^a}{\partial y} + \frac{\partial v_0^a}{\partial x} + \frac{1}{2} \frac{\partial w_0^a}{\partial x} \frac{\partial w_0^a}{\partial y} + \frac{1}{2} \frac{\partial w_0^a}{\partial x} \frac{\partial w_0^a}{\partial y} \right) \right] dx dy = 0, \\ &\int_{\Omega_e} \left(-D_{11}^* \bar{W}_7 M_{xx}^a - D_{12}^* \bar{W}_7 M_{yy}^a + \frac{\partial \bar{W}_7}{\partial x} \frac{\partial w_0^a}{\partial x} \right) dx dy - \oint_{\Gamma_e} \bar{W}_7 \left(n_x \frac{\partial w_0}{\partial x} \right) ds = 0, \\ &\int_{\Omega_e} \left(-D_{12}^* \bar{W}_8 M_{xx}^a - D_{22}^* \bar{W}_8 M_{yy}^a + \frac{\partial \bar{W}_8}{\partial y} \frac{\partial w_0^a}{\partial y} \right) dx dy - \oint_{\Gamma_e} \bar{W}_8 \left(n_y \frac{\partial w_0}{\partial y} \right) ds = 0, \\ &\int_{\Omega_e} \left(-D_{66}^* \bar{W}_9 M_{xy}^a + \frac{\partial \bar{W}_9}{\partial x} \frac{\partial w_0^a}{\partial y} + \frac{\partial \bar{W}_9}{\partial y} \frac{\partial w_0^a}{\partial x} \right) dx dy - \oint_{\Gamma_e} \bar{W}_9 \left(n_x \frac{\partial w_0}{\partial y} + n_y \frac{\partial w_0}{\partial x} \right) ds = 0, \end{aligned} \quad (21)$$

104 All 9 variables are approximated with the Lagrange type interpolation functions, and the
 105 finite element model is of the form

$$\begin{bmatrix} [K^{(11)}] & \dots & [K^{(14)}] & \dots & [K^{(19)}] \\ \vdots & \ddots & \vdots & \ddots & \vdots \\ [K^{(41)}] & \dots & [K^{(44)}] & \dots & [K^{(69)}] \\ \vdots & \ddots & \vdots & \ddots & \vdots \\ [K^{(91)}] & \dots & [K^{(96)}] & \dots & [K^{(99)}] \end{bmatrix} \begin{Bmatrix} \{u_j\} \\ \vdots \\ \{N_j^1\} \\ \vdots \\ \{M_j^3\} \end{Bmatrix} = \begin{Bmatrix} \{F^{(1)}\} \\ \vdots \\ \{F^{(4)}\} \\ \vdots \\ \{F^{(9)}\} \end{Bmatrix}. \quad (22)$$

106 where the coefficients can be easily identified from the weighted-residual statements in (20).

107 **3.4 Finite Element Model III (FSDT)**

108 Model III is based on the following 13 weighed-residual statements of the FSDT:

$$\begin{aligned} & \int_{\Omega_e} \left(\frac{\partial \bar{W}_1}{\partial x} N_{xx}^a + \frac{\partial \bar{W}_1}{\partial y} N_{xy}^a \right) dx dy - \oint_{\Gamma_e} \bar{W}_1 (n_x N_{xx} + n_y N_{xy}) ds = 0, \\ & \int_{\Omega_e} \left(\frac{\partial \bar{W}_2}{\partial x} N_{xy}^a + \frac{\partial \bar{W}_2}{\partial y} N_{yy}^a \right) dx dy - \oint_{\Gamma_e} \bar{W}_2 (n_x N_{xy} + n_y N_{yy}) ds = 0, \\ & \int_{\Omega_e} \left[\frac{\partial \bar{W}_3}{\partial x} Q_x^a + \frac{\partial \bar{W}_3}{\partial y} Q_y^a + \frac{\partial \bar{W}_3}{\partial x} \left(N_{xx}^a \frac{\partial w_0^a}{\partial x} + N_{xy}^a \frac{\partial w_0^a}{\partial y} \right) + \frac{\partial \bar{W}_3}{\partial y} \left(N_{xy}^a \frac{\partial w_0^a}{\partial x} + N_{yy}^a \frac{\partial w_0^a}{\partial y} \right) \right. \\ & \quad \left. - \bar{W}_3 q(x) \right] dx dy \\ & \quad + \oint_{\Gamma_e} \bar{W}_3 \left[\left(Q_x + N_{xx} \frac{\partial w_0}{\partial x} + N_{xy} \frac{\partial w_0}{\partial y} \right) n_x + \left(Q_y + N_{xy} \frac{\partial w_0}{\partial x} + N_{yy} \frac{\partial w_0}{\partial y} \right) n_y \right] ds = 0, \\ & \int_{\Omega_e} \left(\frac{\partial \bar{W}_4}{\partial x} M_{xx}^a + \frac{\partial \bar{W}_4}{\partial y} M_{xy}^a + \bar{W}_4 Q_x^a \right) dx dy + \oint_{\Gamma_e} \bar{W}_4 (M_{xx} n_x + M_{xy} n_y) ds = 0, \\ & \int_{\Omega_e} \left(\frac{\partial \bar{W}_5}{\partial x} M_{xy}^a + \frac{\partial \bar{W}_5}{\partial y} M_{yy}^a + \bar{W}_5 Q_y^a \right) dx dy + \oint_{\Gamma_e} \bar{W}_5 (M_{xy} n_x + M_{yy} n_y) ds = 0, \\ & \int_{\Omega_e} \bar{W}_6 \left\{ -A_{11}^* N_{xx}^a - A_{12}^* N_{yy}^a + \left[\frac{\partial u_0^a}{\partial x} + \frac{1}{2} \left(\frac{\partial w_0^a}{\partial x} \right)^2 \right] \right\} dx dy = 0, \\ & \int_{\Omega_e} \bar{W}_7 \left\{ -A_{12}^* N_{xx}^a - A_{22}^* N_{yy}^a + \left[\frac{\partial v_0^a}{\partial y} + \frac{1}{2} \left(\frac{\partial w_0^a}{\partial y} \right)^2 \right] \right\} dx dy = 0, \\ & \int_{\Omega_e} \bar{W}_8 \left[-A_{66}^* N_{xy}^a + \left(\frac{\partial u_0^a}{\partial y} + \frac{\partial v_0^a}{\partial x} + \frac{1}{2} \frac{\partial w_0^a}{\partial x} \frac{\partial w_0^a}{\partial y} + \frac{1}{2} \frac{\partial w_0^a}{\partial x} \frac{\partial w_0^a}{\partial y} \right) \right] dx dy = 0, \\ & \int_{\Omega_e} \bar{W}_9 \left(-\frac{Q_x^a}{K_s A_{55}} + \frac{\partial w_0^a}{\partial x} + \phi_x^a \right) dx dy = 0, \end{aligned}$$

$$\begin{aligned}
 \int_{\Omega_e} \bar{W}_{10} \left(-\frac{Q_y^a}{K_s A_{44}} + \frac{\partial w_0^a}{\partial y} + \phi_y^a \right) dx dy &= 0, \\
 \int_{\Omega_e} \bar{W}_{11} \left(-D_{11}^* M_{xx}^a - D_{12}^* M_{yy}^a + \frac{\text{partial} \phi_x^a}{\partial x} \right) dx dy &= 0, \\
 \int_{\Omega_e} \bar{W}_{12} \left(-D_{12}^* M_{xx}^a - D_{22}^* M_{yy}^a + \frac{\text{partial} \phi_y^a}{\partial y} \right) dx dy &= 0, \\
 \int_{\Omega_e} \bar{W}_{13} \left(-D_{66}^* M_{xy}^a + \frac{\partial \phi_x^a}{\partial y} + \frac{\partial \phi_y^a}{\partial x} \right) dx dy &= 0.
 \end{aligned} \tag{23}$$

109 where Ω_e and Γ_e denote the element region and its boundary, respectively. The primary
 110 variables and the secondary variable of the Model III can be specified as follows:

	Primary variable	Secondary variable
	u_0	$n_x N_{xx} + n_y N_{xy}$
	v_0	$n_x N_{xy} + n_y N_{yy}$
111	w_0	$V_x n_x + V_y n_y$
	ϕ_x	$M_{xx} n_x + M_{xy} n_y$
	ϕ_y	$M_{xy} n_x + M_{yy} n_y$

112 The finite element model is of the form

$$\begin{bmatrix}
 [K^{(1)(1)}] & \dots & [K^{(1)(7)}] & \dots & [K^{(1)(13)}] \\
 \vdots & \ddots & \vdots & \ddots & \vdots \\
 [K^{(7)(1)}] & \dots & & \dots & [K^{(7)(13)}] \\
 \vdots & \ddots & \vdots & \ddots & \vdots \\
 [K^{(13)(1)}] & \dots & [K^{(13)(6)}] & \dots & [K^{(13)(13)}]
 \end{bmatrix}
 \begin{Bmatrix}
 \{u_j\} \\
 \vdots \\
 \{N_j^2\} \\
 \vdots \\
 \{M_j^3\}
 \end{Bmatrix}
 =
 \begin{Bmatrix}
 \{F^{(1)}\} \\
 \vdots \\
 \{F^{(7)}\} \\
 \vdots \\
 \{F^{(13)}\}
 \end{Bmatrix}. \tag{24}$$

113 The coefficients can be identified with the help of the weighted-residual statements in (23).

114 3.5 Finite Element Model IV (FSDT)

115 The in-plane forces (N_{xx} , N_{xy} and N_{yy}) can be eliminated by substituting from the first two
 116 equilibrium equations into the remaining equations of equilibrium. The weighted-residual
 117 statements of the resulting 10 equations are summarized below:

$$\begin{aligned}
 \int_{\Omega_e} \left\{ \frac{\partial \bar{W}_1}{\partial x} \left[A_{11} \left(\frac{\partial u_0^a}{\partial x} + \frac{1}{2} \left(\frac{\partial w_0^a}{\partial x} \right)^2 \right) + A_{12} \left(\frac{\partial v_0^a}{\partial y} + \frac{1}{2} \left(\frac{\partial w_0^a}{\partial y} \right)^2 \right) \right] \right. \\
 \left. + \frac{\partial \bar{W}_1}{\partial y} \left[A_{66} \left(\frac{\partial u_0^a}{\partial y} + \frac{\partial v_0^a}{\partial x} + \frac{\partial w_0^a}{\partial x} \frac{\partial w_0^a}{\partial y} \right) \right] \right\} dx dy - \oint_{\Gamma_e} \bar{W}_1 (n_x N_{xx} + n_y N_{xy}) ds = 0, \\
 \int_{\Omega_e} \left\{ \frac{\partial \bar{W}_2}{\partial y} \left[A_{12} \left(\frac{\partial u_0^a}{\partial x} + \frac{1}{2} \left(\frac{\partial w_0^a}{\partial x} \right)^2 \right) + A_{22} \left(\frac{\partial v_0^a}{\partial y} + \frac{1}{2} \left(\frac{\partial w_0^a}{\partial y} \right)^2 \right) \right] \right. \\
 \left. + \frac{\partial \bar{W}_2}{\partial x} \left[A_{66} \left(\frac{\partial u_0^a}{\partial y} + \frac{\partial v_0^a}{\partial x} + \frac{\partial w_0^a}{\partial x} \frac{\partial w_0^a}{\partial y} \right) \right] \right\} dx dy - \oint_{\Gamma_e} \bar{W}_2 (n_x N_{xy} + n_y N_{yy}) ds = 0,
 \end{aligned} \tag{118}$$

$$\begin{aligned}
 & \int_{\Omega_e} \left[\frac{\partial \bar{W}_3}{\partial x} Q_x^a + \frac{\partial \bar{W}_3}{\partial y} Q_y^a + \frac{\partial \bar{W}_3}{\partial x} \frac{\partial w_0^a}{\partial x} \left[A_{11} \left(\frac{\partial u_0^a}{\partial x} + \frac{1}{2} \left(\frac{\partial w_0^a}{\partial x} \right)^2 \right) + A_{12} \left(\frac{\partial v_0^a}{\partial y} + \frac{1}{2} \left(\frac{\partial w_0^a}{\partial y} \right)^2 \right) \right] \right. \\
 & \quad + \frac{\partial \bar{W}_3}{\partial x} \frac{\partial w_0^a}{\partial y} \left[A_{66} \left(\frac{\partial u_0^a}{\partial y} + \frac{\partial v_0^a}{\partial x} + \frac{\partial w_0^a}{\partial x} \frac{\partial w_0^a}{\partial y} \right) \right] \\
 & \quad + \frac{\partial \bar{W}_3}{\partial y} \frac{\partial w_0^a}{\partial x} \left[A_{66} \left(\frac{\partial u_0^a}{\partial y} + \frac{\partial v_0^a}{\partial x} + \frac{\partial w_0^a}{\partial x} \frac{\partial w_0^a}{\partial y} \right) \right] \\
 & \quad + \frac{\partial \bar{W}_3}{\partial y} \frac{\partial w_0^a}{\partial y} \left[A_{12} \left(\frac{\partial u_0^a}{\partial x} + \frac{1}{2} \left(\frac{\partial w_0^a}{\partial x} \right)^2 \right) + A_{22} \left(\frac{\partial v_0^a}{\partial y} + \frac{1}{2} \left(\frac{\partial w_0^a}{\partial y} \right)^2 \right) \right] \\
 & \quad \left. - \bar{W}_3 q(x) \right] dx dy \\
 & + \oint_{\Gamma_e} \bar{W}_3 \left[\left(Q_x + N_{xx} \frac{\partial w_0}{\partial x} + N_{xy} \frac{\partial w_0}{\partial y} \right) n_x + \left(Q_y + N_{xy} \frac{\partial w_0}{\partial x} + N_{yy} \frac{\partial w_0}{\partial y} \right) n_y \right] ds = 0, \\
 \\
 & \int_{\Omega_e} \left(\frac{\partial \bar{W}_4}{\partial x} M_{xx}^a + \frac{\partial \bar{W}_4}{\partial y} M_{xy}^a + \bar{W}_4 Q_x^a \right) dx dy + \oint_{\Gamma_e} \bar{W}_4 (M_{xx} n_x + M_{xy} n_y) ds = 0, \\
 & \int_{\Omega_e} \left(\frac{\partial \bar{W}_5}{\partial x} M_{xy}^a + \frac{\partial \bar{W}_5}{\partial y} M_{yy}^a + \bar{W}_5 Q_y^a \right) dx dy + \oint_{\Gamma_e} \bar{W}_5 (M_{xy} n_x + M_{yy} n_y) ds = 0, \\
 & \int_{\Omega_e} \bar{W}_6 \left(-\frac{Q_x^a}{K_s A_{55}} + \frac{\partial w_0^a}{\partial x} + \phi_x^a \right) dx dy = 0, \\
 & \int_{\Omega_e} \bar{W}_7 \left(-\frac{Q_y^a}{K_s A_{44}} + \frac{\partial w_0^a}{\partial y} + \phi_y^a \right) dx dy = 0, \\
 & \int_{\Omega_e} \bar{W}_8 \left(-D_{11}^* M_{xx}^a - D_{12}^* M_{yy}^a + \frac{\partial \phi_x^a}{\partial x} \right) dx dy = 0, \\
 & \int_{\Omega_e} \bar{W}_9 \left(-D_{12}^* M_{xx}^a - D_{22}^* M_{yy}^a + \frac{\partial \phi_y^a}{\partial y} \right) dx dy = 0, \\
 & \int_{\Omega_e} \bar{W}_{10} \left(-D_{66}^* M_{xy}^a + \frac{\partial \phi_x^a}{\partial y} + \frac{\partial \phi_y^a}{\partial x} \right) dx dy = 0. \tag{25}
 \end{aligned}$$

119 The primary and the secondary variables of Model IV are the same as in Model III. The
 120 finite element model is of the form

$$\begin{bmatrix} [K^{(1)(1)}] & \dots & [K^{(1)(7)}] & \dots & [K^{(1)(10)}] \\ \vdots & \ddots & \vdots & \ddots & \vdots \\ [K^{(5)(1)}] & \dots & & \dots & [K^{(5)(10)}] \\ \vdots & \ddots & \vdots & \ddots & \vdots \\ [K^{(10)(1)}] & \dots & [K^{(10)(6)}] & \dots & [K^{(10)(10)}] \end{bmatrix} \begin{Bmatrix} \{u_j\} \\ \vdots \\ \{p_j^2\} \\ \vdots \\ \{M_j^3\} \end{Bmatrix} = \begin{Bmatrix} \{F^{(1)}\} \\ \vdots \\ \{F^{(5)}\} \\ \vdots \\ \{F^{(10)}\} \end{Bmatrix}. \tag{26}$$

121 where the nonzero coefficients are

$$\begin{aligned}
 [K^{11}] &= \int_{\Omega_e} \left\{ A_{11} \frac{\partial \psi_i^{u_0}}{\partial x} \frac{\partial \psi_j^{u_0}}{\partial x} + A_{66} \frac{\partial \psi_i^{u_0}}{\partial y} \frac{\partial \psi_j^{u_0}}{\partial y} \right\} dx dy \\
 [K^{12}] &= \int_{\Omega_e} \left\{ A_{12} \frac{\partial \psi_i^{u_0}}{\partial x} \frac{\partial \psi_j^{v_0}}{\partial y} + A_{66} \frac{\partial \psi_i^{u_0}}{\partial y} \frac{\partial \psi_j^{v_0}}{\partial x} \right\} dx dy \\
 [K^{13}] &= \frac{1}{2} \int_{\Omega_e} \left\{ \frac{\partial \psi_i^{u_0}}{\partial x} \left(A_{11} \frac{\partial \mathbf{w}_0^a}{\partial \mathbf{x}} \frac{\partial \psi_j^{w_0}}{\partial x} + A_{12} \frac{\partial \mathbf{w}_0^a}{\partial \mathbf{y}} \frac{\partial \psi_j^{w_0}}{\partial y} \right) + A_{66} \frac{\partial \psi_i^{u_0}}{\partial y} \left(\frac{\partial \mathbf{w}_0^a}{\partial \mathbf{x}} \frac{\partial \psi_j^{w_0}}{\partial y} + \frac{\partial \mathbf{w}_0^a}{\partial \mathbf{y}} \frac{\partial \psi_j^{w_0}}{\partial x} \right) \right\} dx dy \\
 [K^{22}] &= \int_{\Omega_e} \left\{ A_{22} \frac{\partial \psi_i^{v_0}}{\partial y} \frac{\partial \psi_j^{v_0}}{\partial y} + A_{66} \frac{\partial \psi_i^{v_0}}{\partial x} \frac{\partial \psi_j^{v_0}}{\partial x} \right\} dx dy \\
 [K^{21}] &= \int_{\Omega_e} \left\{ A_{12} \frac{\partial \psi_i^{v_0}}{\partial y} \frac{\partial \psi_j^{u_0}}{\partial x} + A_{66} \frac{\partial \psi_i^{v_0}}{\partial x} \frac{\partial \psi_j^{u_0}}{\partial y} \right\} dx dy \\
 [K^{23}] &= \frac{1}{2} \int_{\Omega_e} \left\{ \frac{\partial \psi_i^{v_0}}{\partial y} \left(A_{22} \frac{\partial \mathbf{w}_0^a}{\partial \mathbf{y}} \frac{\partial \psi_j^{w_0}}{\partial y} + A_{12} \frac{\partial \mathbf{w}_0^a}{\partial \mathbf{x}} \frac{\partial \psi_j^{w_0}}{\partial x} \right) + A_{66} \frac{\partial \psi_i^{v_0}}{\partial x} \left(\frac{\partial \mathbf{w}_0^a}{\partial \mathbf{x}} \frac{\partial \psi_j^{w_0}}{\partial y} + \frac{\partial \mathbf{w}_0^a}{\partial \mathbf{y}} \frac{\partial \psi_j^{w_0}}{\partial x} \right) \right\} dx dy \\
 [K^{31}] &= \int_{\Omega_e} \left\{ \frac{\partial \psi_i^{w_0}}{\partial x} \left(A_{11} \frac{\partial \mathbf{w}_0^a}{\partial \mathbf{x}} \frac{\partial \psi_j^{u_0}}{\partial x} + A_{66} \frac{\partial \mathbf{w}_0^a}{\partial \mathbf{y}} \frac{\partial \psi_j^{u_0}}{\partial y} \right) + \frac{\partial \psi_i^{w_0}}{\partial y} \left(A_{66} \frac{\partial \mathbf{w}_0^a}{\partial \mathbf{x}} \frac{\partial \psi_j^{u_0}}{\partial y} + A_{12} \frac{\partial \mathbf{w}_0^a}{\partial \mathbf{y}} \frac{\partial \psi_j^{u_0}}{\partial x} \right) \right\} dx dy \\
 [K^{32}] &= \int_{\Omega_e} \left\{ \frac{\partial \psi_i^{w_0}}{\partial y} \left(A_{22} \frac{\partial \mathbf{w}_0^a}{\partial \mathbf{y}} \frac{\partial \psi_j^{v_0}}{\partial y} + A_{66} \frac{\partial \mathbf{w}_0^a}{\partial \mathbf{x}} \frac{\partial \psi_j^{v_0}}{\partial x} \right) + \frac{\partial \psi_i^{w_0}}{\partial x} \left(A_{66} \frac{\partial \mathbf{w}_0^a}{\partial \mathbf{y}} \frac{\partial \psi_j^{v_0}}{\partial x} + A_{12} \frac{\partial \mathbf{w}_0^a}{\partial \mathbf{x}} \frac{\partial \psi_j^{v_0}}{\partial y} \right) \right\} dx dy \\
 [K^{33}] &= \frac{1}{2} \int_{\Omega_e} \left\{ \left[A_{11} \left(\frac{\partial \mathbf{w}_0^a}{\partial \mathbf{x}} \right)^2 + A_{66} \left(\frac{\partial \mathbf{w}_0^a}{\partial \mathbf{y}} \right)^2 \right] \frac{\partial \psi_i^{w_0}}{\partial x} \frac{\partial \psi_j^{w_0}}{\partial x} \right. \\
 &\quad \left. + \left[A_{66} \left(\frac{\partial \mathbf{w}_0^a}{\partial \mathbf{x}} \right)^2 + A_{22} \left(\frac{\partial \mathbf{w}_0^a}{\partial \mathbf{y}} \right)^2 \right] \frac{\partial \psi_i^{w_0}}{\partial y} \frac{\partial \psi_j^{w_0}}{\partial y} \right. \\
 &\quad \left. + (A_{12} + A_{66}) \frac{\partial \mathbf{w}_0^a}{\partial \mathbf{x}} \frac{\partial \mathbf{w}_0^a}{\partial \mathbf{y}} \left(\frac{\partial \psi_i^{w_0}}{\partial x} \frac{\partial \psi_j^{w_0}}{\partial y} + \frac{\partial \psi_i^{w_0}}{\partial y} \frac{\partial \psi_j^{w_0}}{\partial x} \right) \right\} dx dy \\
 [K^{36}] &= \int_{\Omega_e} \left\{ \frac{\partial \psi_i^{w_0}}{\partial x} \psi_j^{Q_x} \right\} dx dy & [K^{37}] &= \int_{\Omega_e} \left\{ \frac{\partial \psi_i^{w_0}}{\partial y} \psi_j^{Q_y} \right\} dx dy \\
 aaa [K^{66}] &= \int_{\Omega_e} \left\{ -\frac{\psi_i^{Q_x} \psi_j^{Q_x}}{(K_s A_{55})} \right\} dx dy & [K^{63}] &= \int_{\Omega_e} \left\{ \psi_i^{Q_x} \frac{\partial \psi_j^{w_0}}{\partial x} \right\} dx dy \\
 [K^{64}] &= \int_{\Omega_e} \left\{ \psi_i^{Q_x} \psi_j^{\phi_x} \right\} dx dy & [K^{75}] &= \int_{\Omega_e} \left\{ \psi_i^{Q_y} \psi_j^{\phi_y} \right\} dx dy \\
 [K^{77}] &= \int_{\Omega_e} \left\{ -\frac{\psi_i^{Q_y} \psi_j^{Q_y}}{(K_s A_{44})} \right\} dx dy & [K^{73}] &= \int_{\Omega_e} \left\{ \psi_i^{Q_y} \frac{\partial \psi_j^{w_0}}{\partial y} \right\} dx dy \\
 [K^{88}] &= \int_{\Omega_e} \left\{ -D_{11}^* \psi_i^{M_{xx}} \psi_j^{M_{xx}} \right\} dx dy & [K^{89}] &= \int_{\Omega_e} \left\{ -D_{12}^* \psi_i^{M_{xx}} \psi_j^{M_{yy}} \right\} dx dy \\
 [K^{84}] &= \int_{\Omega_e} \left\{ \psi_i^{M_{xx}} \frac{\partial \psi_j^{\phi_x}}{\partial x} \right\} dx dy & [K^{95}] &= \int_{\Omega_e} \left\{ \psi_i^{M_{yy}} \frac{\partial \psi_j^{\phi_y}}{\partial y} \right\} dx dy \\
 [K^{98}] &= \int_{\Omega_e} \left\{ -D_{12}^* \psi_i^{M_{yy}} \psi_j^{M_{xx}} \right\} dx dy & [K^{99}] &= \int_{\Omega_e} \left\{ -D_{22}^* \psi_i^{M_{yy}} \psi_j^{M_{yy}} \right\} dx dy \\
 [K^{(10)4}] &= \int_{\Omega_e} \left\{ \psi_i^{M_{xy}} \frac{\partial \psi_j^{\phi_x}}{\partial y} \right\} dx dy & [K^{(10)5}] &= \int_{\Omega_e} \left\{ \psi_i^{M_{xy}} \frac{\partial \psi_j^{\phi_y}}{\partial x} \right\} dx dy \\
 [K^{(10)(10)}] &= \int_{\Omega_e} \left\{ -D_{66}^* \psi_i^{M_{xy}} \psi_j^{M_{xy}} \right\} dx dy
 \end{aligned}$$

$$\begin{aligned}
 \{F^1\} &= \oint_{\Gamma_e} \psi_i^u \{n_x N_{xx} + n_y N_{xy}\} ds, & \{F^2\} &= \oint_{\Gamma_e} \psi_i^{v_0} \{n_x N_{xy} + n_y N_{yy}\} ds, \\
 \{F^3\} &= \int_{\Omega_e} \{\psi_i^{w_0} q(x)\} dx dy + \oint_{\Gamma_e} \psi_i^{w_0} [(V_x) n_x + (V_y) n_y] ds, \\
 \{F^4\} &= \oint_{\Gamma_e} \psi_i^{\phi_x} \{M_{xx} n_x + M_{xy} n_y\} ds, & \{F^5\} &= \oint_{\Gamma_e} \psi_i^{\phi_y} \{M_{xy} n_x + M_{yy} n_y\} ds, \quad (27)
 \end{aligned}$$

4 NUMERICAL RESULTS

In this section we will discuss the numerical results obtained with the finite element models developed in Section 3. Comparisons of various models are presented with linear and nonlinear solutions available in the literature. The Newton’s iterative technique is used to solve the nonlinear equations. The tangent stiffness coefficients are computed from the stiffness coefficients (see Reddy [6] for details).

We consider a square plate with the following material properties:

$$\begin{aligned}
 a = b = 10 \text{ in, } h = 1 \text{ in, } E = 7.8 \times 10^6 \text{ psi,} \\
 \nu = 0.3 \text{ (or 0.25 for linear analysis)}
 \end{aligned} \quad (28)$$

Due to the biaxial symmetry of the geometry, boundary conditions, and applied load, only a quadrant of the plate was used as the computational domain. Three types of boundary conditions are considered with common boundary conditions along the symmetry lines of the quadrant. The specific boundary conditions are shown in Fig. 2.

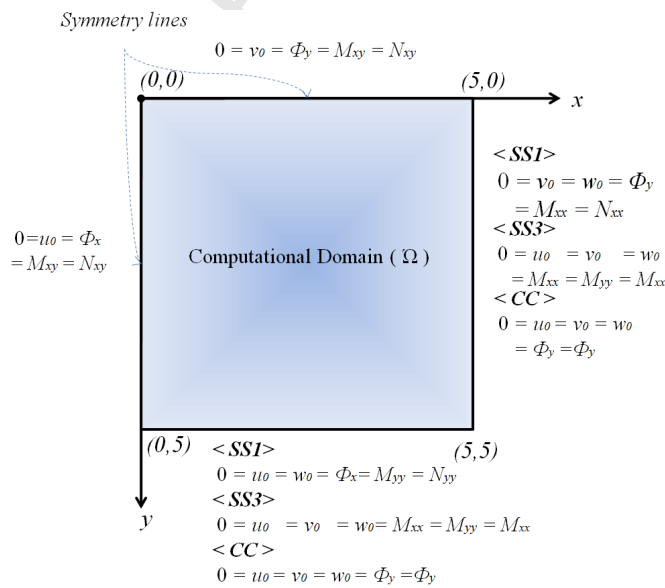


Figure 2 Boundary and symmetry conditions in a quadrant of the square plate.

135 4.1 Linear analysis

136 To verify the accuracy of the newly developed plate bending models, solutions obtained with
 137 the new models are compared with those of the existing models [1, 2, 6] and analytic solutions.
 138 First, the linear solutions of the mixed CPT models will be discussed by comparing the results
 139 obtained with displacement based model [4, 6].

140 The comparison of the results of the various models under the simple support I (SS1) and
 141 clamped (CC) boundary conditions are given in the Table 1 and 2. For the simple support
 142 boundary condition (SS1), Model II showed best accuracy for the center vertical deflection,
 143 while Model I provided better accuracy for the center bending moment, as shown in the Table
 144 1. For the clamped (CC) boundary condition, the Model I showed best accuracy both for
 145 the center vertical deflection and the center bending moment as shown in the Table 2. By
 146 including the shear forces (i.e., V_x and V_y) as nodal values in Model I, more accurate center
 147 bending moment and center vertical deflection were obtained.

Table 1 Comparison of the linear solution of various CPT Models, isotropic ($\nu = 0.3$) square plate, simple supported (SS1).

Mesh size	Current Models		Mixed Reddy [4]	Mixed Herrmann [2]	Hybrid Allman [1]	Compatible cubic displacement Model [6]
	Model I	Model II				
Liner (4-node)	Center deflection (* equivalent quadratic), $\bar{w} = w \times D_{11} \times 10^2 / (q_0 \times a^4)$ (Exact solution, 0.4062 [4])					
1×1	0.4613 (* -)	0.4613 (-)	0.4613	0.9018	0.347	0.220
2×2	0.4383 (0.4154)	0.4237 (0.4154)	0.4237	0.5127	0.392	0.371
4×4	0.4135 (0.4067)	0.4106 (0.4067)	0.4106	0.4316	0.403	0.392
6×6	0.4094 (0.4063)	0.4082 (0.4063)	0.4082	0.4172	-	-
8×8	0.4079 (0.4063)	0.4073 (0.4063)	-	-	-	-
Liner (4-node)	Center bending moment (equivalent quadratic), $\bar{M} = M \times 10 / (q_0 \times a^2)$ (Exact solution, 0.479 [4])					
1×1	0.7196 (-)	0.7196 (-)	0.7196	0.328	0.604	-
2×2	0.5029 (0.4906)	0.5246 (0.4096)	0.5246	0.446	0.515	-
4×4	0.4850 (0.4797)	0.4892 (0.4796)	0.4892	0.471	0.487	-
6×6	0.4816 (0.4790)	0.4834 (0.4790)	0.4834	0.476	-	-
8×8	0.4804 (0.4788)	0.4814 (0.4789)	-	-	-	-

148 Current CPT mixed models were compared with the displacement based model. For the
 149 CPT displacement based model, non-conforming and the conforming [6] elements should be
 150 used because of the continuity requirement of the weak formulation. Current mixed models
 151 provided better accuracy when the compatible nine-node quadratic element was used. Even the
 152 four-node liner element also provided acceptable accuracy compared with the non-conforming
 153 displacement based model. The stresses obtained from the current mixed models showed better
 154 accuracy, because the stresses can be directly computed by using bending moment or shear
 155 resultant obtained at a node.

Table 2 Comparison of the linear solution of various CPT Models, isotropic ($\nu = 0.3$) square plate, clamped (CC).

Mesh size	Current Models		Mixed Reddy [4]	Mixed Herrmann [2]	Hybrid Allman [1]	Compatible cubic displacement Model [6]
	Model I	Model II				
Liner (4-node)	Center deflection (* equivalent quadratic), $\bar{w} = w \times D_{11} \times 10^2 / (q_0 \times a^4)$ (Exact solution, 0.1265 [4])					
1x1	0.1576 (* -)	1.6644 (-)	1.6644	0.7440	0.087	0.026
2x2	0.1502 (0.1512)	0.1528 (0.1512)	0.1528	0.2854	0.132	0.120
4x4	0.1310 (0.1279)	0.1339 (0.1278)	0.1339	0.1696	0.129	0.121
6x6	0.1284 (0.1268)	0.1299 (0.1268)	0.1299	0.1463	-	-
8x8	0.1265 (0.1265)	0.1270 (0.1266)	-	-	-	-
Liner (4-node)	Center bending moment (equivalent quadratic), $\bar{M} = M \times 10 / (q_0 \times a^2)$ (Exact 0.230 [4])					
1x1	0.4918 (-)	0.5193 (-)	0.5193	0.208	0.344	-
2x2	0.2627 (0.2552)	0.3165 (0.2552)	0.3165	0.242	0.314	-
4x4	0.2354 (0.2312)	0.2478 (0.2310)	0.2478	0.235	0.250	-
6x6	0.2318 (0.2295)	0.2374 (0.2295)	0.2374	0.232	-	-
8x8	0.2286 (0.2290)	0.2310 (0.2291)	-	-	-	-

156 Next, the numerical results of the Model III and IV are compared with the results of
 157 Reddy's mixed model [4] in Table 3. The mixed model developed by Reddy [4] included
 158 bending moments as independent nodal value in the finite element model, while current Model
 159 III and IV included vertical shear resultants (i.e., Q_x and Q_y), as independent nodal value.
 160 Note that the difference between Model III and VI comes from the presence or absence of
 161 membrane forces (i.e., N_{xx} , N_{yy} and N_{xy}) in the finite element models. Thus, the solution of
 162 the linear bending of each model is essentially the same as shown in the Table 3.

Table 3 Comparison of the current mixed FSDT linear solution with that of the other mixed model (Reddy [4]), with isotropic ($\nu = 0.25$, $K_s = 5/6$) square plate, simple supported (SS1).

Mesh size	Current Models		Mixed Reddy [4]	Current Models		Mixed Reddy [4]
	Model(III)	Model(IV)		Model III	Model IV	
Liner (4-node)	Center deflection, $\bar{w} = w D_{11} \times 10^2 / (q_0 a^4)$, (Exact 0.427 [5])			Center bending moment $\bar{M} = M \times 10 / (q_0 a^2)$, (Exact 0.479 [5])		
1x1	0.4174 (* -)	0.4174 (-)	0.4264	0.6094 (-)	0.6094 (-)	0.6094
2x2	0.4293 (0.4345)	0.4293 (0.4345)	0.4321	0.5060 (0.4779)	0.5060 (0.4779)	0.5070
4x4	0.4280 (0.4277)	0.4280 (0.4277)	0.4285	0.4849 (0.4779)	0.4849 (0.4779)	0.4850
8x8	0.4275 (0.4273)	0.4275 (0.4273)	-	0.4803 (0.4785)	0.4803 (0.4785)	-

163 4.2 Nonlinear analysis

164 A total of 12 load steps were used with the following values of the load parameter
 165 $P = q_0 a^4 / (E_{22} h^4)$:

$$P = \{ 6.25, 12.5, 25.0, 25.0, 25.0, 25.0, 25.0, 25.0, 25.0, 25.0, 25.0, 25.0 \} \quad (29)$$

166 A tolerance $\epsilon = 0.01$ was used for convergence in the Newton's iteration scheme. Model I
 167 and II was compared with the CPT displacement base model to see its non-linear behavior.
 168 The center deflection, w_0 , of the newly developed models are presented in the Table 4. In every
 169 load step, the converged solution was obtained within 4 iterations. Results of full integration
 170 and the reduced integration are presented in Table 4. In both models both membrane and
 171 shear locking are not severe, as judged against the published solutions, and the effect of reduced
 172 integration is not significant.

Table 4 Effect of reduced integration in Model I and II.

$P = \frac{q_0 a^4}{(E_{22} h^4)}$	Center deflection, w, CPT-(SS1)							
	MODEL I				MODEL II			
	4x4-Linear		2x2-Quadratic		4x4-Linear		2x2-Quadratic	
	FI	RI	FI	RI	FI	RI	FI	RI
6.25	0.2736	0.2737	0.2691	0.2691	0.2718	0.2719	0.2691	0.2691
12.50	0.5090	0.5096	0.5005	0.5007	0.5059	0.5064	0.5005	0.5007
25.00	0.8608	0.8629	0.8468	0.8475	0.8565	0.8579	0.8470	0.8476
50.00	1.3119	1.3163	1.2923	1.2943	1.3061	1.3093	1.2932	1.2947
75.00	1.6185	1.6244	1.5960	1.5997	1.6114	1.6157	1.5977	1.6004
100.00	1.8572	1.8641	1.8328	1.8383	1.8488	1.8539	1.8357	1.8394
125.00	2.0559	2.0637	2.0302	2.0377	2.0462	2.0521	2.0339	2.0391
150.00	2.2280	2.2365	2.2011	2.2107	2.2171	2.2235	2.2059	2.2125
175.00	2.3811	2.3900	2.3529	2.3649	2.3689	2.3757	2.3588	2.3669
200.00	2.5196	2.5289	2.4901	2.5045	2.5062	2.5133	2.4971	2.5068
225.00	2.6465	2.6562	2.6158	2.6327	2.6320	2.6394	2.6240	2.6352
250.00	2.7641	2.7741	2.7321	2.7515	2.7484	2.7561	2.7414	2.7541

173 The nonlinear load vs. deflection and load vs. stress are presented in Fig. 3. For the SS3
 174 boundary condition, both vertical deflection and stresses of Models I and II showed very close
 175 agreement with the displacement finite element model. The normal stresses and the membrane
 176 stresses were computed at points $(0, 0, 0.5h)$ and $(0, 0, 0)$, respectively. The 9-node quadratic
 177 element mesh showed closer agreement with the displacement FSDT model.

178 The nonlinear center deflection, normal and membrane stresses of Models I and II are
 179 compared with the results of the displacement model. The results are presented in the Table
 180 5. A 4×4 mesh of nine-node element showed the closest agreement with the displacement FSDT

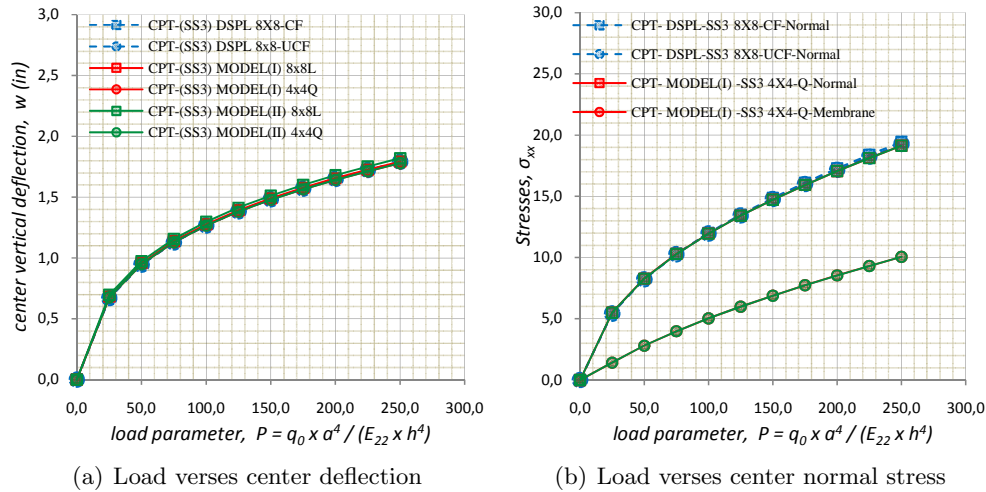


Figure 3 Plots of the membrane and normal stress of Model I, II and CPT displacement model under SS3 boundary condition.

181 model, as shown in Fig. 4. To see the convergence of the various models, center deflections
 182 of previously developed models with 2x2 quadratic and 4x4 linear meshes under SS1 and SS3
 183 boundary conditions are compared in Table 6. Every model showed good convergence with a
 184 tolerance $\epsilon = 0.01$, except for the Model IV. The Model IV showed acceptable convergence with
 185 SS3 boundary condition but with SS1 boundary condition it took slightly more iterations to
 186 converge. This is due to the fact that plates with SS1 boundary conditions are more flexible
 187 and exhibit greater nonlinearity.

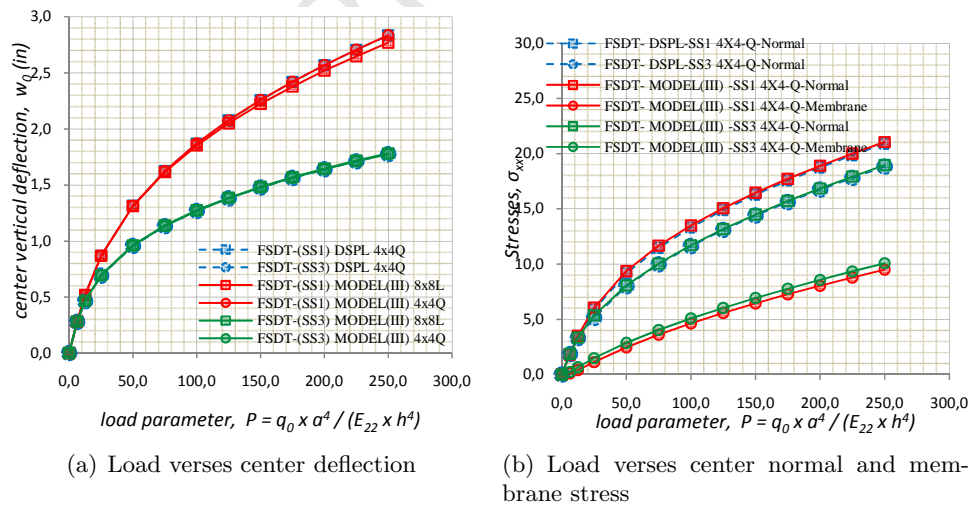


Figure 4 Plots of the center deflection, normal and membrane stress of Model III with that of the FSDT displacement model under SS1 and SS3 boundary conditions.

Table 5 Comparison of the center deflection and normal stress of Model I and II with the CPT displacement model.

$P = \frac{q_0 a^4}{(E_{22} h^4)}$	Center deflection, w , CPT-(SS3)					
	MODEL I		MODEL II		DSPL	DSPL
	8×8-L	4×4-Q	8×8-L	4×4-Q	8×8-CF	8×8-UCF
0.00	0.0000	0.0000	0.0000	0.0000	0.0000	0.0000
25.00	0.6836	0.6774	0.6966	0.6771	0.6690	0.6700
50.00	0.9581	0.9501	0.9743	0.9497	0.9450	0.9460
75.00	1.1388	1.1296	1.1572	1.1293	1.1270	1.1280
100.00	1.2775	1.2675	1.2977	1.2672	1.2670	1.2680
125.00	1.3919	1.3813	1.4137	1.3809	1.3830	1.3830
150.00	1.4902	1.4791	1.5134	1.4787	1.4830	1.4830
175.00	1.5770	1.5654	1.6015	1.5650	1.5710	1.5710
200.00	1.6552	1.6432	1.6809	1.6428	1.6510	1.6510
225.00	1.7265	1.7142	1.7533	1.7138	1.7240	1.7240
250.00	1.7923	1.7796	1.8201	1.7793	1.7910	1.7910
$P = \frac{q_0 a^4}{(E_{22} h^4)}$	Normal stresses, $\sigma_{xx}^{normal} (0, 0, 0.5h) \times a^2/E_{11}$, CPT-(SS3)					
	MODEL I		MODEL II		DSPL	DSPL
	8×8-L	4×4-Q	8×8-L	4×4-Q	8×8-CF	8×8-UCF
0.00	0.0000	0.0000	0.0000	0.0000	0.0000	0.0000
25.00	5.5195	5.5008	5.3402	5.4980	5.4260	5.4230
50.00	8.2751	8.2782	8.0297	8.2741	8.2470	8.2270
75.00	10.2633	10.2937	9.9885	10.2901	10.3090	10.2710
100.00	11.8988	11.9589	11.6072	11.9541	12.0170	11.9610
125.00	13.2682	13.4106	13.0238	13.4098	13.5130	13.4400
150.00	14.6077	14.7273	14.3036	14.7196	14.8670	14.7770
175.00	15.8033	15.9322	15.4838	15.9311	16.1170	16.0090
200.00	16.8734	17.0628	16.5872	17.0613	17.2870	17.1620
225.00	17.8924	18.1308	17.6290	18.1271	18.3930	18.2510
250.00	18.9188	19.1385	18.6199	19.1411	19.4460	19.2870

188 The distributions of various quantities are presented in the Figs. 5 and 6. The data was
189 post-processed inside of each element using 10 Gauss points ranging from -0.975 to 0.975,
190 for both newly developed models (i.e., Models I and III) and FSDT displacement model.
191 Converged solutions of SS3 at load parameter $P = 250.0$ are used for the post processing.

192 Even though all models show similar patterns for each variable as shown in the Fig. 5,
193 one may note that the contour plots obtained from the current mixed models offer better
194 accuracy at the boundaries of the elements, while the plots obtained from the displacement
195 based model show discontinuous distributions. Obviously, the plots in Figs. 6 and 4.6 show

Table 6 Comparison of the convergence of Model I, II, III and IV under the SS1 and SS3 boundary conditions.

$P = \frac{q_0 a^4}{(E_{22} h^4)}$	Center deflection, w (*iteration times to converge), SS1 various models					
	Model (III)		Model (IV)		Model (I)	Model (II)
	4x4-L	2x2-Q	4x4-L	2x2-Q	2x2-Q	2x2-Q
0.00	0.0000(3)	0.0000(3)	0.0000(3)	0.0000(3)	0.0000(3)	0.0000(3)
6.25	0.2821(3)	0.2816(3)	0.2877(3)	0.2847(3)	0.2691(3)	0.2691(3)
12.50	0.5213(3)	0.5195(3)	0.5281(5)	0.5233(5)	0.5007(3)	0.5007(4)
25.00	0.8730(3)	0.8695(3)	0.8801(6)	0.8736(6)	0.8475(3)	0.8476(4)
50.00	1.3195(3)	1.3187(3)	1.3237(7)	1.3169(7)	1.2943(3)	1.2947(3)
75.00	1.6228(3)	1.6282(3)	1.6302(7)	1.6256(7)	1.5997(3)	1.6004(3)
100.00	1.8589(3)	1.8720(3)	1.8684(7)	1.8663(7)	1.8383(3)	1.8394(3)
125.00	2.0553(3)	2.0769(2)	2.0682(7)	2.0688(7)	2.0377(3)	2.0391(3)
150.00	2.2251(3)	2.2552(2)	2.2420(6)	2.2456(6)	2.2107(3)	2.2125(3)
175.00	2.3757(3)	2.4141(2)	2.3914(6)	2.3973(6)	2.3649(3)	2.3669(2)
200.00	2.5116(3)	2.5580(2)	2.5308(6)	2.5392(6)	2.5045(2)	2.5068(2)
225.00	2.6376(2)	2.6898(2)	2.6592(6)	2.6704(6)	2.6327(2)	2.6352(2)
250.00	2.7521(2)	2.8117(2)	2.7717(5)	2.7850(5)	2.7515(2)	2.7541(2)

$P = \frac{q_0 a^4}{(E_{22} h^4)}$	Center deflection, w (*iteration times to converge), SS3 various models					
	Model (III)		Model (IV)		Model (I)	Model (II)
	4x4-L	2x2-Q	4x4-L	2x2-Q	2x2-Q	2x2-Q
0.00	0.0000	0.0000	0.0000	0.0000	0.000	0.000
6.25	0.2911(4)	0.2865(4)	0.2912(4)	0.2866(4)	0.2718(4)	0.2713(4)
12.50	0.4779(3)	0.4709(3)	0.4784(3)	0.4716(3)	0.4561(3)	0.4552(3)
25.00	0.7076(3)	0.6978(3)	0.7080(3)	0.6982(3)	0.6872(3)	0.6860(3)
50.00	0.9763(3)	0.9626(3)	0.9760(4)	0.9622(4)	0.9578(3)	0.9563(4)
75.00	1.1542(3)	1.1375(3)	1.1535(4)	1.1367(4)	1.1360(3)	1.1345(4)
100.00	1.2914(3)	1.2724(3)	1.2908(4)	1.2715(4)	1.2730(3)	1.2714(4)
125.00	1.4050(2)	1.3841(2)	1.4046(4)	1.3832(4)	1.3861(3)	1.3845(4)
150.00	1.5030(2)	1.4803(2)	1.5015(3)	1.4783(3)	1.4834(2)	1.4818(3)
175.00	1.5897(2)	1.5655(2)	1.5885(3)	1.5636(3)	1.5693(2)	1.5678(3)
200.00	1.6679(2)	1.6422(2)	1.6669(3)	1.6405(3)	1.6467(2)	1.6452(3)
225.00	1.7393(2)	1.7124(2)	1.7385(3)	1.7107(3)	1.7173(2)	1.7159(3)
250.00	1.8054(2)	1.7773(2)	1.8047(3)	1.7757(3)	1.7825(2)	1.7811(3)

196 that the distributions of stresses and bending moments of Model III are relatively more accurate
 197 than those computed in the displacement model of FSDT, even though bending moments of
 198 Model III have some oscillations at the inter-element boundary. Of course, the displacement
 199 models exhibit even higher discontinuities in the bending moments as well as shear forces.

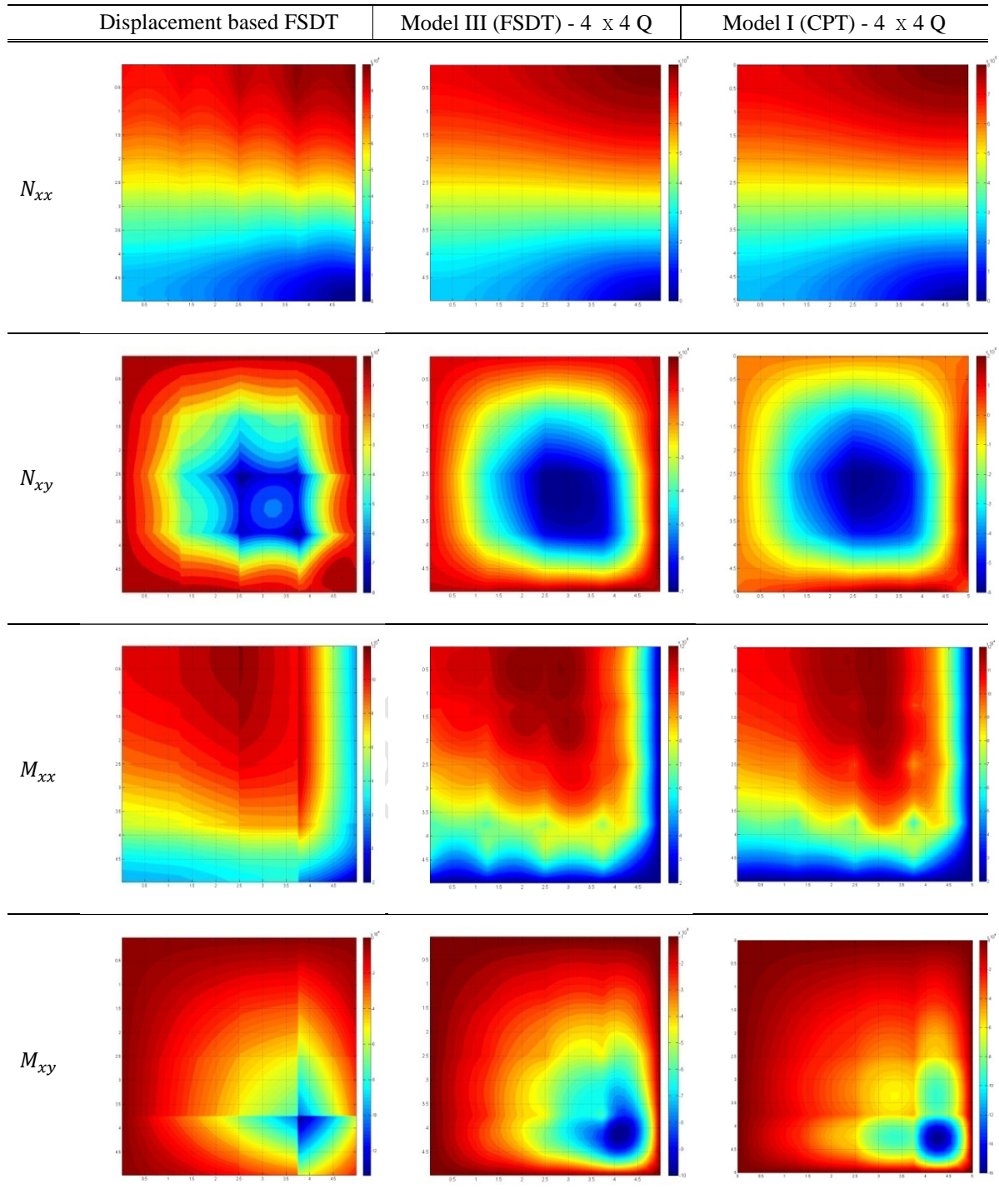


Figure 5 Post processed quadrant images of the variables in various models, SS3, with converged solution at load parameter $\bar{P} = 250$.

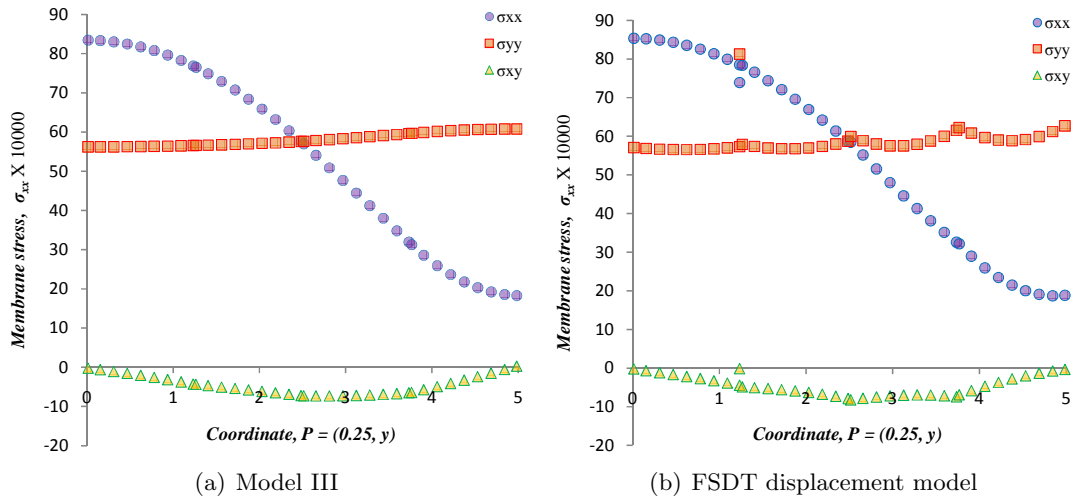


Figure 6 Plots of the non-linear membrane stresses of Model III and FSDT displacement model along the $x = 2.5$.

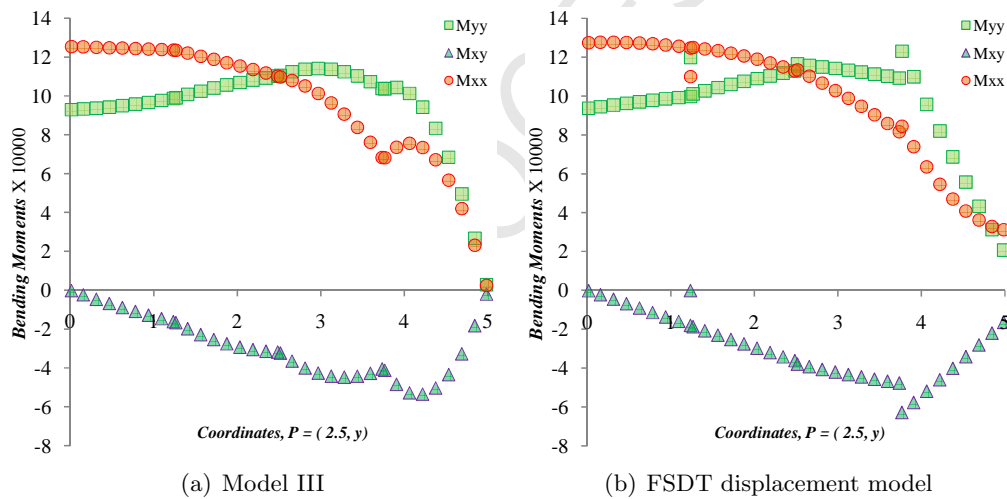


Figure 7 Plots of the non-linear bending moments of Model III and FSDT displacement model along the $x = 2.5$.

200 **5 CONCLUSIONS**

201 In this study, advantages and disadvantages of newly developed nonlinear finite element models
 202 of plate bending are investigated. In almost every case, newly developed mixed plate bending
 203 models provided better accuracy for linear and nonlinear solutions of deflections and stress
 204 resultants. Model IV showed poor convergence compared with other models because of the
 205 absence of typical displacement variables. An important observation of the present study is
 206 that the mixed models do not experience significant locking.

207 In summary, the two main advantages of the mixed model are the reduction in the continuity

208 requirements for the transverse deflection in CPT and the increase of the accuracy for the stress
209 resultants. Of course, there is a slight increase in computational cost due to the increased
210 number of degrees of freedom per node.

211 **Acknowledgement.** The second author gratefully acknowledges the support of this research
212 by Army Research Office is gratefully acknowledged.

213 References

- 214 [1] D. J. Allman. Triangular finite element for plate bending with constant and linearly varying bending moments. *High*
215 *Speed Computing of Elastic Structures I*, pages 106–136, 1971.
- 216 [2] L. R. Herrmann. Finite element bending analysis for plates. *J. Engng. Mech. Div. , ASCE*, 93(EM5), 1967.
- 217 [3] N. S. Putcha and J. N. Reddy. A refined mixed shear flexible finite element for the nonlinear analysis of laminated
218 plates. *Computers & Structures*, 22(4):529–538, 1986.
- 219 [4] J. N. Reddy. Mixed finite element models for laminated composite plate. *Journal of Engineering for Industry*,
220 109:39–45, 1987.
- 221 [5] J. N. Reddy. *Energy Principles and Variational Methods in Applied Mechanics*. John Wiley & Sons, New York, 2
222 edition, 2002.
- 223 [6] J. N. Reddy. *An Introduction to Nonlinear Finite Element Analysis*. Oxford University Press, Oxford, New York,
224 2004.
- 225 [7] J. N. Reddy. *Mechanics of Laminated Composite Plates and Shells : Theory and Analysis*. CRC Press, Boca Raton,
226 2 edition, 2004.
- 227 [8] J. N. Reddy. *An Introduction to the Finite Element Method*. McGraw-Hill, New York, 3 edition, 2006.
- 228 [9] J. N. Reddy. *Theory and Analysis of Elastic Plates and Shells*. CRC Press, Boca Raton, FL, 2007.
- 229 [10] J. N. Reddy. *An Introduction to Continuum Mechanics with Applications*. Cambridge University Press, New York,
230 2008.